



THEORETICAL AND EXPERIMENTAL STUDIES OF THERMAL  
STRATIFICATION IN HOT AND COLD POOLS OF PFBR

K. Velusamy, G. Titus, A. Rajakumar, G. Ravichandran,  
G. Padmakumar, G. Vaidyanathan, R.D. Kale, S.C. Chetal  
and S.B. Bhoje

Reactor Group  
Indira Gandhi Centre for Atomic Research  
Kalpakkam 603 102 INDIA

ABSTRACT

Results of experimental studies carried out in two water models of size 1/24 and 1/15, to assess the free level fluctuation in the hot pool of PFBR are presented. The results when extrapolated to the prototype gives a ripple height of 50 mm. The results of thermal stratification studies carried out in 1/24 scale model, using hot and cold water indicates that the interface velocity can be correlated with the Richardson number. The paper also gives the details of computer codes developed for the estimation of flow and temperature fields in the pools.

1.0 INTRODUCTION

A 500 MWe sodium cooled, pool type, Prototype Fast Breeder Reactor (PFBR) is currently under design in India. Sodium enters the core at 380 °C and exits from the core at different temperatures ranging from 400 °C in the shielding subassemblies to 550 °C in the fuel subassemblies. The mixed mean temperature of hot sodium is 530 °C. While improper mixing of the sodium streams from different subassemblies leads to thermal fluctuations on the bottom of the control plug, the imperfect mixing in the hot pool along with continuous heat loss from hot pool to cold pool results in thermal stratification under steady state operation. These stratified layers fluctuate with a frequency governed by the level fluctuations of the free level. During a reactor scram due to power failure, the inertia of the

fluid coming out of the core becomes comparable to the buoyancy forces existing in the hot pool and this again leads to thermal stratification. As time progresses, the hot-cold interface moves up. All the above phenomena lead to thermal stresses in the primary circuit components dipped in sodium, in the reactor vessel. This paper presents the details of theoretical models used in the analysis of the above phenomena, studies carried out and some experiments carried out to validate the predictions.

2.0 COMPUTER CODES

Initially a computer code THYC-2D for two dimensional axisymmetric analysis was developed[1] and applied for scoping studies. Subsequently a three dimensional code THYC-3D was developed on similar lines[2]. The major features of the codes are given below:

- cartesian or cylindrical coordinate systems
- uniform or non-uniform grids
- steady state or transient
- temperature dependent variable density or Boussinesq approximation
- pressure velocity coupling through SIMPLE Algorithm[3]
- upwind/hybrid/power law schemes to combine convection & diffusion terms
- line by line or plane by plane or whole field solver
- traversing, marching, sweeping in any direction
- turbulent flows simulated by using constant turbulent viscosity and conductivity model or K- epsilon model
- porous body formulations to take care of submerged components

- conjugate heat transfer option

The codes solve the basic conservation equations of mass, momentum and energy for single phase fluids. These equations are cast into a generalised conservative equation of the form

$$\frac{\delta(\rho\phi)}{\delta t} + \text{div.}(\rho V\phi) = \text{div.}(\Gamma_{\phi} \text{grad } \phi) + S_{\phi}$$

The four terms in the above equations are the unsteady term, convection term, diffusion term and source term.  $\phi$  is the dependent variable e.g. velocity, temperature,  $\rho$  is density,  $V$  is velocity vector and  $\Gamma_{\phi}$  is the diffusion coefficient.

The process of discretisation is carried out using the control volume based discretisation method<sup>[3]</sup>. Staggered grids have been followed wherein the velocities are defined at the mid point of the faces of the control volume, while temperature and pressure are defined at the grid points.

The fluxes due to convection and diffusion are evaluated at the control volume faces, in terms of upstream and downstream nodal values. There is no separate equation for pressure and it is indirectly specified through continuity equation. When the correct pressure field is substituted into the momentum equation, the resulting velocity field satisfies the continuity equation.

The discretised equation for a variable defined at any grid point is derived by integrating the conservation equation over the control volume around that grid point and over an elemental time interval. The general form of the discretised equation is given below:

$$a_{ijk} \phi_{ijk} = b_{ijk} \phi_{i+1,jk} + c_{ijk} \phi_{i-1,jk} + d_{ijk} \phi_{ij+1,k} + f_{ijk} \phi_{ij-1,k} + g_{ijk} \phi_{ijk+1} + h_{ijk} \phi_{ijk-1} + l_{ijk}$$

where a,b,c,d,f,g,h and l are the coefficients of the equation.

These algebraic sets of equations are solved by any one of the methods viz. line by line, plane by plane, or whole field procedures which are extensions of the basic Thomas Algorithm<sup>[3]</sup>.

The solutions are obtained by using problem dependent relaxation procedures<sup>[4]</sup> and convergence is declared by checking the normalised residue values for all the variables to satisfy the error tolerance limit specified for each variable.

The computer codes have been tested with several standard problems like flow in a driven cavity, flow development in a straight circular pipe, natural convection in a square box and horizontal cylindrical annulus etc. The predictions have been found to be satisfactory. Details are reported elsewhere<sup>[2]</sup>.

### 3.0 STEADY STATE

The flow and temperature fields have been analysed in the hot and cold pools of PFBR using the two dimensional code. The flow through the control plug is 12 %. The schematic diagram and boundary conditions are shown in Fig 1. IHX primary inlet windows and pumps were simulated through sink terms in the continuity equation, while flows leaving IHX primary outlet and control plug skirt were treated as specified internal boundary conditions.

The temperature field in the hot and cold pools at 100 % and

20 % power is given in Figs 2 and 3. For 100 %, it is clear that in the hot pool, the cavity between the inner vessel and shielding assemblies is highly stratified. This is because the hot fluid recirculation is confined to the top of the cavity and heat loss is continuously taking place through the lower shell of the inner vessel to the cold pool. In the cold pool, the region between the redan of inner vessel and main vessel baffles is stratified. For 20 % load case the hot pool below the level of control plug is highly stratified and so also the cold pool below the redan as exemplified by horizontal temperature contours. From these studies the thermal loading on inner vessel, control plug etc. have been obtained.

#### 4.0 TRANSIENT

The transient studied refers to reactor trip without and with loss of flow. The temperature field in the hot pool without loss of core flow is presented in Fig. 4 to 6 for  $t = 10, 50$  and  $100$  s. It is seen that stratified sodium layers are present in the upper part of the hot pool. The cold front has moved upto the bottom of control plug in  $150$  s. Fig. 7 to 9 show the temperature fields at  $t = 10, 50$  and  $100$  s in the hot pool with loss of flow. It can be seen that thermal stratification is of a higher degree as compared to the case without loss of flow. The cold front movement is very slow and is advantageous in subjecting the control plug parts to a lesser thermal shock during a reactor scram. These studies have resulted in design intent to reduce the core flow to a minimum value along with a reactor trip. The temperature fluctuations in the hot pool just above IHX windows

is shown in Fig. 10, for a case without loss of core flow. It can be seen that the hot sodium temperature fluctuates upto about  $100$  s while the cold sodium temperature continuously decreases.

#### 5.0 DECAY HEAT REMOVAL CONDITION

The transient benchmark experiment "RAMONA" conducted at Karlsruhe has provided data for the parametric variation of temperatures and flows in the hot pool during transition from power to natural convection condition<sup>[7]</sup>. In simulation of the experiment the hot pool and cold pool were modelled using THYC-2D, while a one dimensional representation is used for IHX, immersion cooler and pump. The thermal stratification in the hot pool at the HT 2.3 tree position is indicated by the vertical temperature profiles shown in Fig 11 at different times. Comparison between the the calculations and experiments is good.

#### 6.0 EXPERIMENTS ON SCALE MODELS

Two scale models have been constructed in perspex for simulation of the hot pool of PFBR. Water is used as the simulant fluid and control plug is non-permeable. The first model is of  $1/24$  scale where only the flow through fuel assemblies has been simulated. In the other model of  $1/15$  scale, the geometric simulation is better and the core, blanket, peripheral subassembly flows have been simulated. The dimensionless thermal hydraulic parameters which characterise the process are Froude, Reynolds, Peclet and Richardson numbers. They represent the effect of gravity, viscosity, heat transfer and buoyancy compared with flow momentum.

### 6.1 Velocity Measurements

Initially steady state flow pattern in the hot pool were studied at different flows, arrived at based on Froude similarity. The velocities were measured in the x,y and z directions using a 3 mm miniature propeller type anemometer with directional sensitivity. This step was done to assess the computer code THYC for hydraulic predictions. Fig. 12a shows the comparison between the measured and predicted axial velocities, Fig. 12b shows similar comparison for radial velocities. It can be seen that there is a good comparison. The differences can be attributed to the correlations used in the codes for representation of the pressure drop in the region between core top and bottom of control plug.

### 6.2 Level Fluctuation Studies

With fluctuations of the free level, the components dipped in the hot pool will experience alternatively hot sodium at 530°C and argon at about 300 °C. This will introduce fatigue stresses at the region close to free level where the temperatures are in the creep range. To assess the level fluctuations, measurements were carried out with a conductance probe. The level variation results in change of conductance between two stainless steel rods of 3 mm diameter separated by 3 mm. The conductance change is measured with an electronic circuitry comprising a Wienbridge oscillator, amplifier and rectifier. It was seen that the ripple height varied from about 0.2 mm near the control plug to 0.4 mm near IHX in 1/24 scale model. Level fluctuations measured in 1/15 scale model showed higher values than those in the 1/24 scale

model. The ripple height varied from 2 mm near control plug to 3.5 mm near the IHX. From this, it can be concluded that ripple height in the prototype would be around 45 to 50 mm. The power spectral density obtained through FFT analysis is shown in Fig. 13 for a location midway between control plug and IHX.

The above data is useful for fatigue analysis of the hot pool components like inner vessel, control plug, pump standpipe etc. which are affected by stratification. The thermally stratified region moves up and down with the level fluctuations. The structural analysis of PFBR inner vessel due to free level fluctuations shows acceptable ripple heights of 110 mm<sup>[8]</sup>.

### 6.3 Thermal Stratification Experiments

During a reactor scram, cooler fluid comes out of the core and enters the hot pool which is at a higher temperature. With lower velocities a stage comes when the fluid is not able to overcome the buoyancy forces and stratified layers are formed, leading to significant axial gradient of temperature in the hot pool structures. As time passes the cold hot interface moves up causing thermal fatigue, as this interface fluctuates continuously. The studies are carried out in the 1/24 scale model by using hot water (80 °C) and cold water (30 °C). The model is initially filled with hot water flowing continuously and then cold water at a reduced flow rate is introduced to simulate a power failure with reactor scram. The temperatures in the hot pool are acquired using a thermocouple rack connected to a data acquisition system. To study the effect of different cold flow

rates the same was varied from 10 % to 100 %. A typical temperature evolution obtained at 20 % flow is shown in Fig. 14. The temperature of hot water for different cold flows were determined using Richardson similitude between model and prototype. The interface velocity (non-dimensionalised) was correlated with Ri number as  $V = 0.0015 Ri^{-0.8}$ . The analysis of the results showed that as long as the Reynolds number is greater than 20,000 there is no effect of it on the interface velocity. Tanaka et. al. [9] have reported a value of 10,000. It was seen that the characteristic velocity used by them for Reynolds number is the mean core velocity while in this case it is the subassembly outlet velocity. With the change in the characteristic velocity the Reynolds number in the present experiment is also close to 10,000.

The comparison of the predictions by THYC-2D code with the measurements is shown in Fig 15. Here the temperature variation with time at different heights is plotted. It can be seen that there is a fair match.

Studies are planned in larger 1/15 scale model and 1/8 scale models in hot and cold plena.

## 7.0 SUMMARY

This paper has brought out the theoretical and experimental studies in the areas of thermal stratification during steady state and transients. The level fluctuations govern the frequency of oscillation of the stratified layers and the same has been obtained from experiments. Further analysis and experiments are planned in cold plenum.

## REFERENCES

1. Velusamy K, Rajakumar A, Vaidyanathan G, Bhoje S.B., Thermal Hydraulic Analysis in the Design of Inner Vessel, Proc. 4th Conf. Liquid Metal Engg. Tech., Avignon, (1988).
2. Asok Kumar M. et al, THYC-3D A Computer Code for Thermal Hydraulic Analysis, Proc. 4th Int. Conf. on Simulation Methods in Nuc. Engg., Montreal, Canada, June (1993).
3. Patankar S.V., Numerical Heat Transfer and Fluid Flow, McGraw Hill, New York (1980).
4. Anil Lal S. et al, Software Development for LMFBR Thermal Hydraulics in Engg. Software, Editors, C.V. Ramakrishnan, A. Varadarajan, C.S. Desai, Narosa Publishing House, New Delhi, (1989).
5. Anil Lal S. et al, Transient Evolution of Temperature in Parts of the Control Plug Within Hotpool, 11th National Heat & Mass Transfer Conference, Madras, India Dec. (1991).
6. Chellapandi P. et al, Structural Integrity Evaluation of PFBR Control Plug, 11 SMiRT, Japan, Aug (1991).
7. D. Weinberg et al, Investigation of Thermal Hydraulics on Transition from Forced to Natural Convection in RAMONA EFR Project (1990).
8. R. Ramesh et al., Structural integrity Evaluation of Thin vessels under temperature fluctuations and variations near sodium free level, Paper to this meeting. 9. Tanaka N., Moriya S., Fujimoro K., Thermal Hydraulic Characteristics in Reactor Vessel of Pool Type Fast Breeder, 2nd Int. Top Meeting on Nuc. Power Plant Thermal Hyd. and Operation, Tokyo, (1986).

FILE : PAP1

Fig. 1 Schematic Diagram and Boundary Conditions

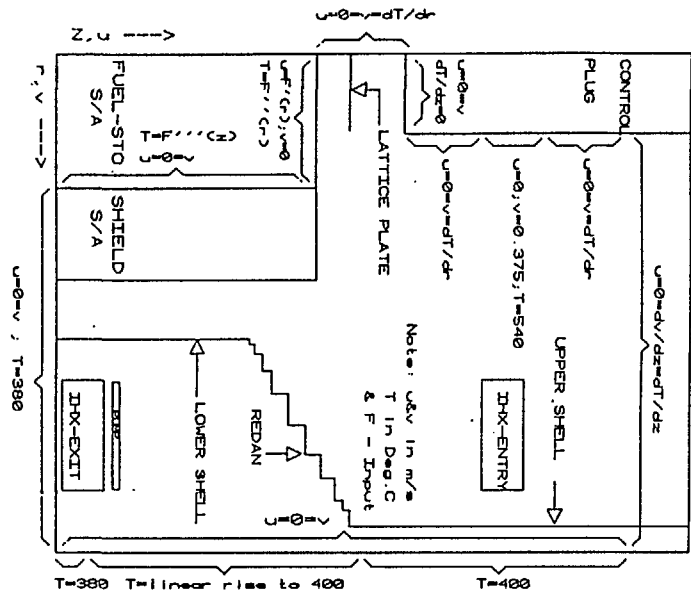


Fig. 2 Temperature Field in the Pools (100% Power)

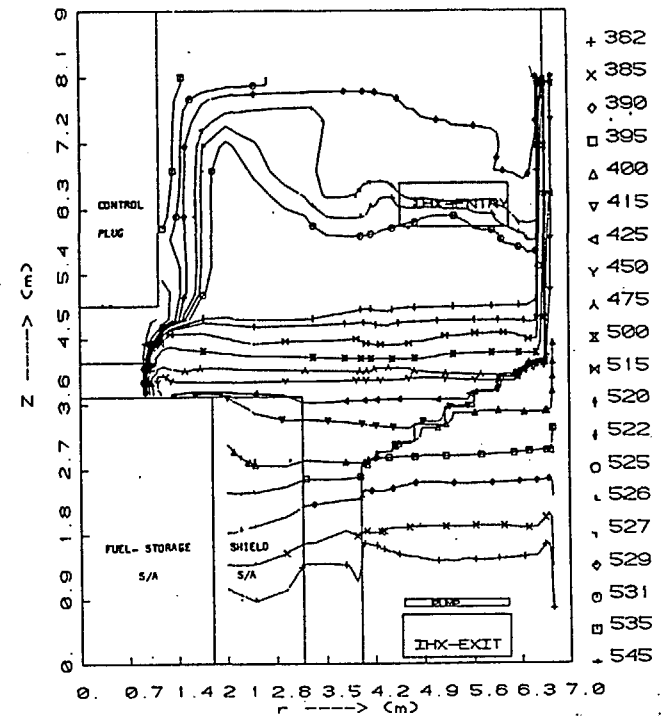
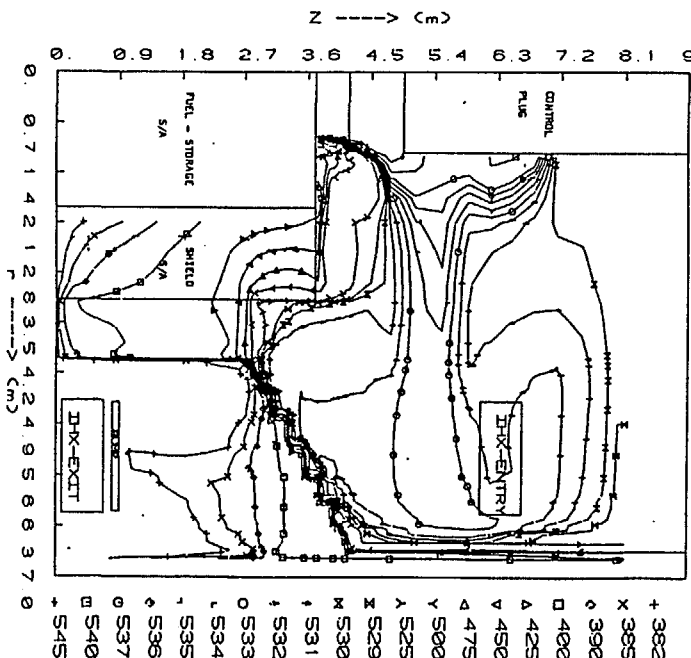


Fig. 3 Temperature Field in the Pools (20% Power)

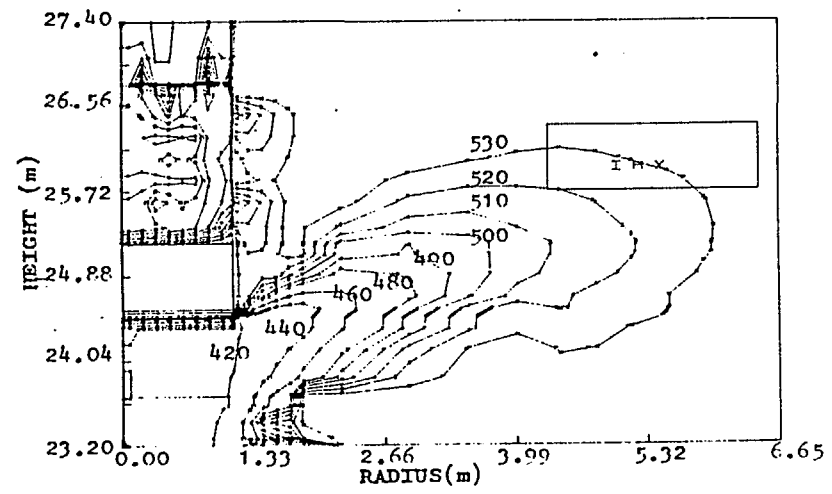


Fig. 4 Transient Temperature Field in the Hot Pool (t=10s; without loss of flow)

118

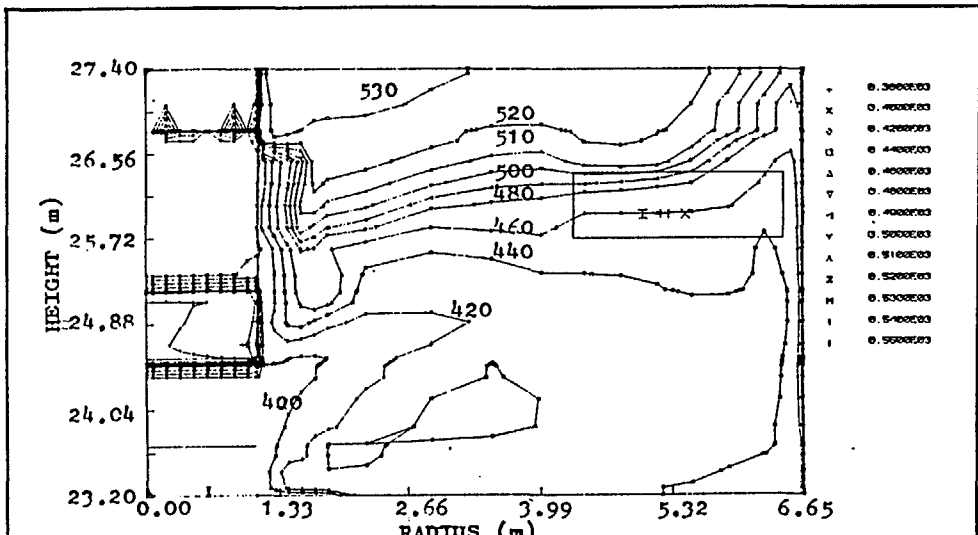


Fig. 5 Transient Temperature Field in the Hot Pool  
(t = 50 s; without loss of flow)

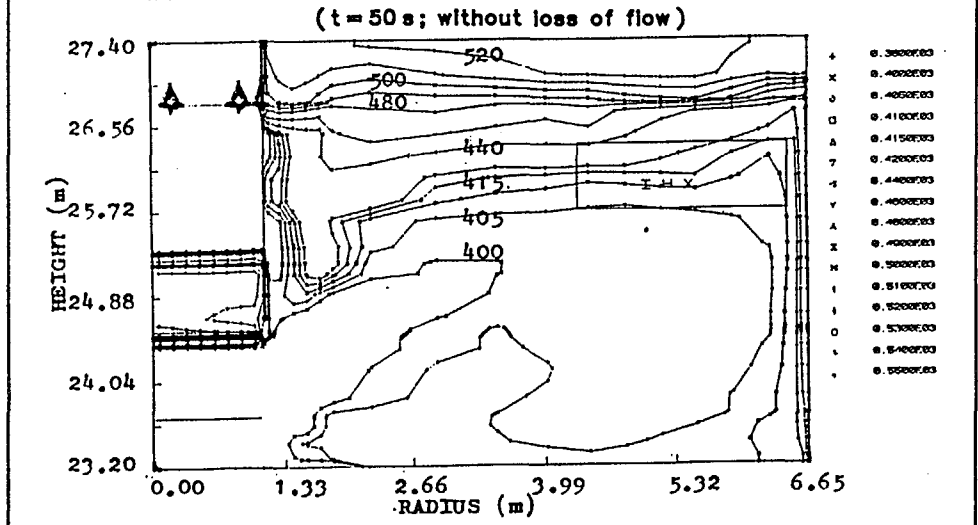


Fig. 6 Transient Temperature Field in the Hot Pool  
(t = 100 s; without loss of flow)

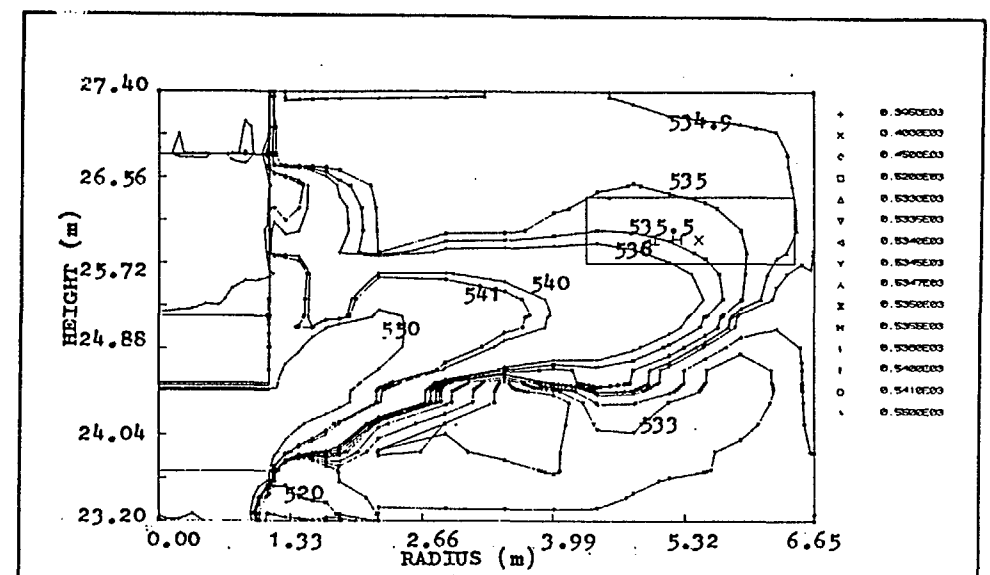


Fig. 7 Transient Temperature Field in the Hot Pool  
(t = 10 s; with loss of flow)

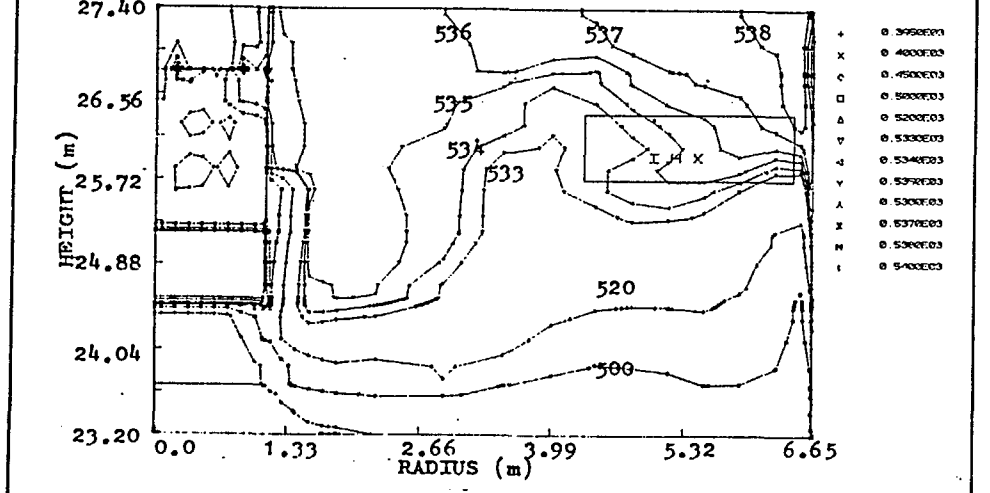


Fig. 8 Transient Temperature Field in the Hot Pool  
(t = 50 s; with loss of flow)

119

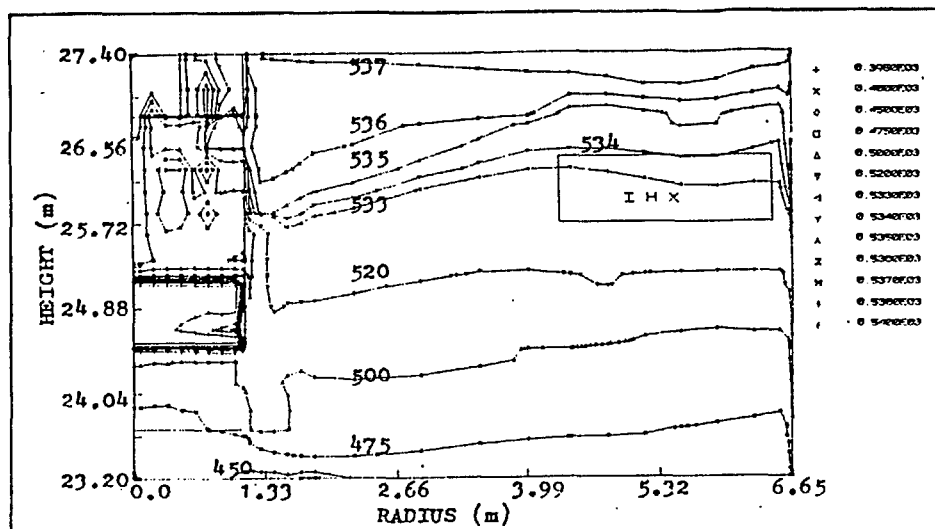


Fig. 9 Transient Temperature Field in the Hot Pool  
( $t = 100$  s; with loss of flow)

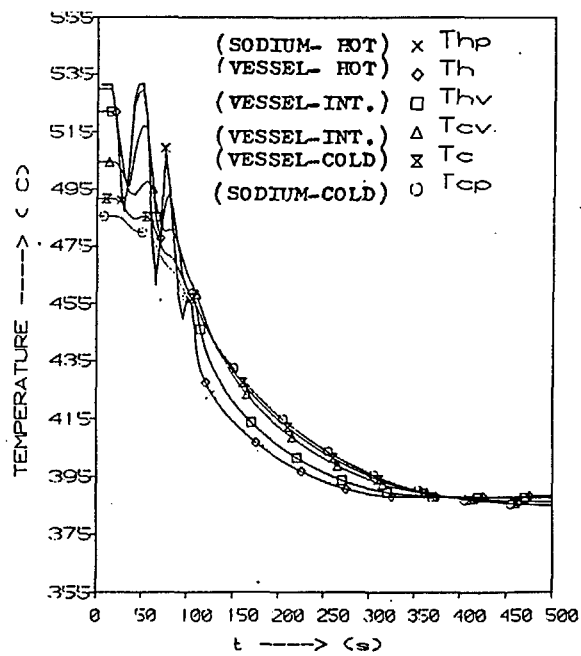


Fig. 10 Temperature Fluctuations in the Hot Pool  
(above IHX Inlet; without loss of flow)

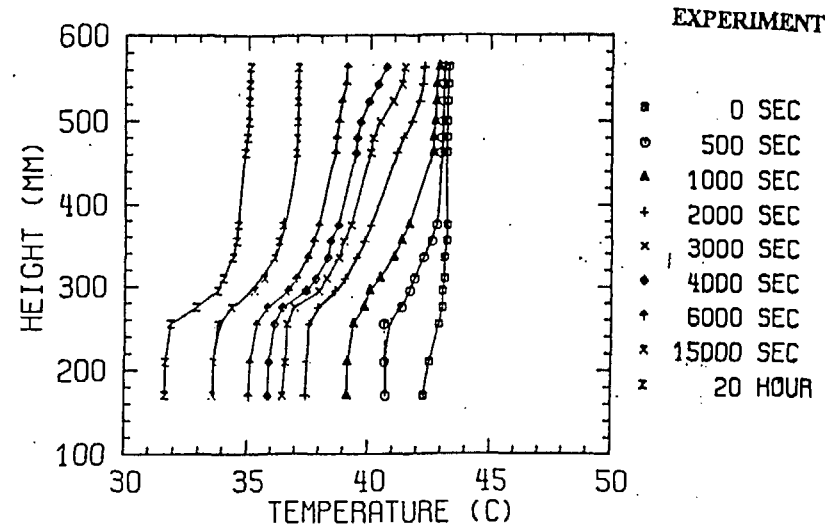


Fig. 11a Hot Pool Axial Temperature Distribution  
in RAMONA (Experiment)

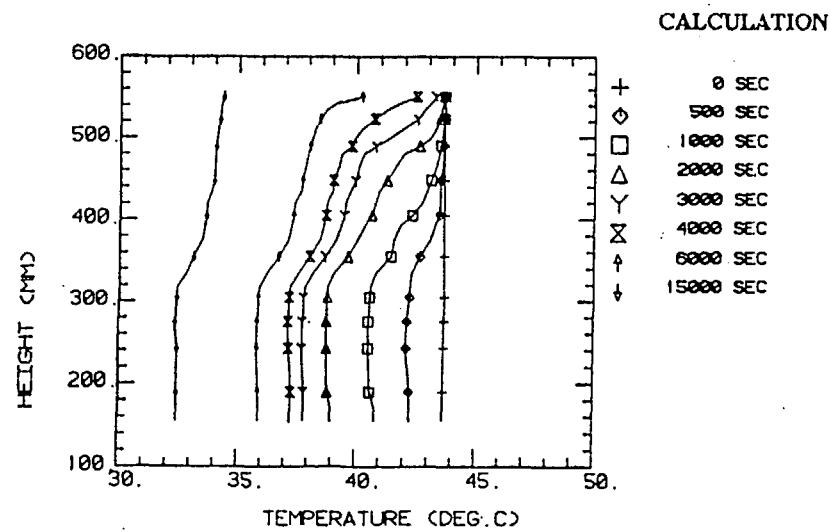
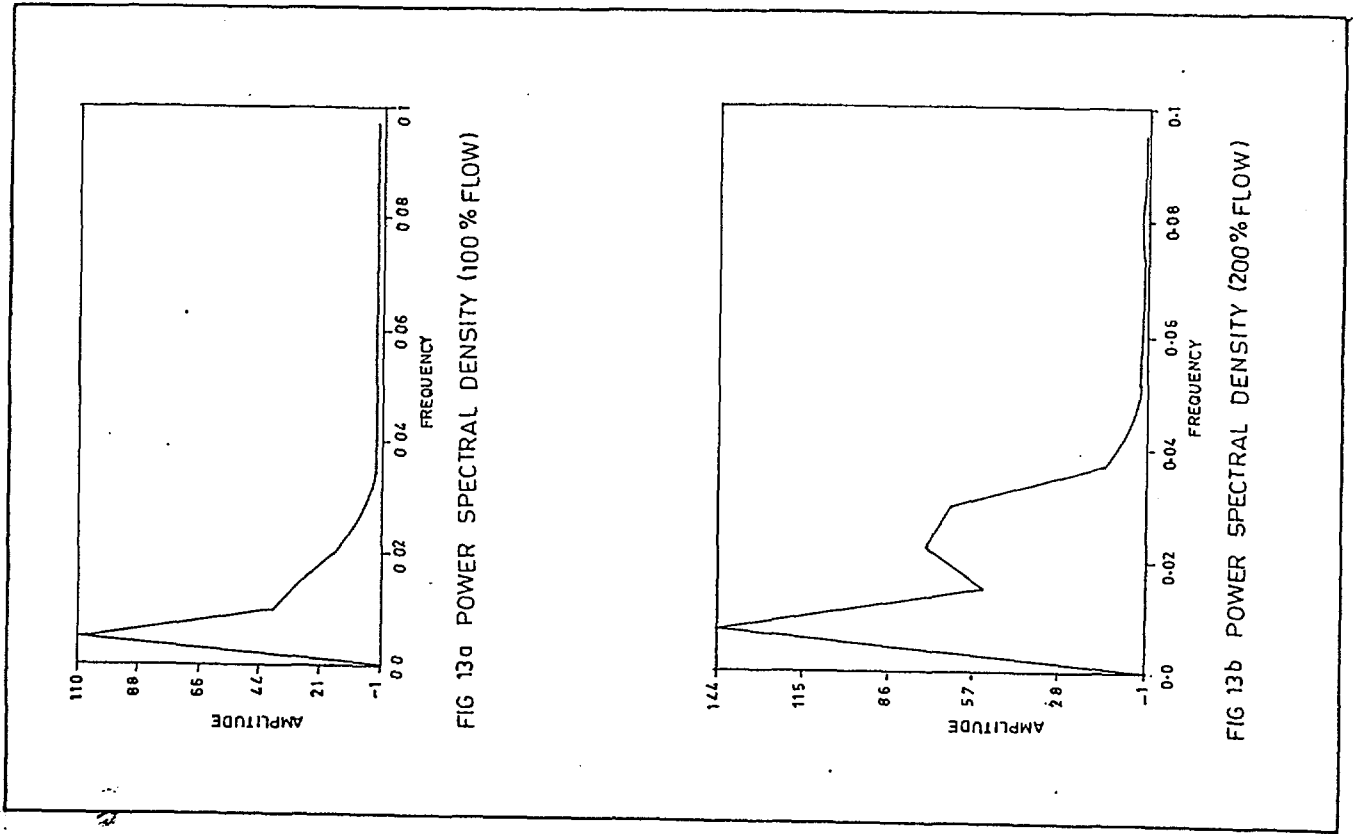
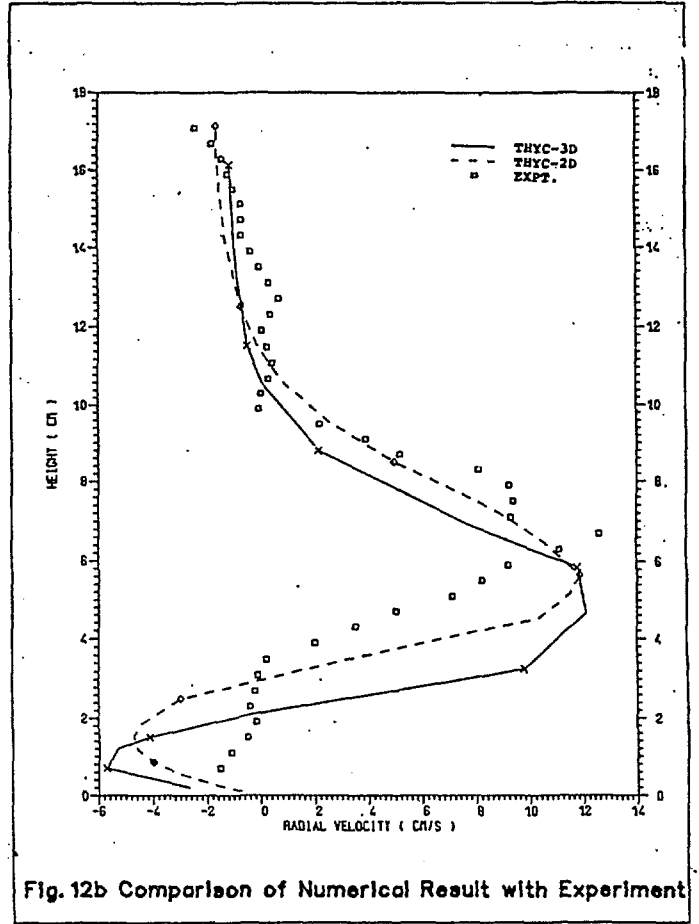
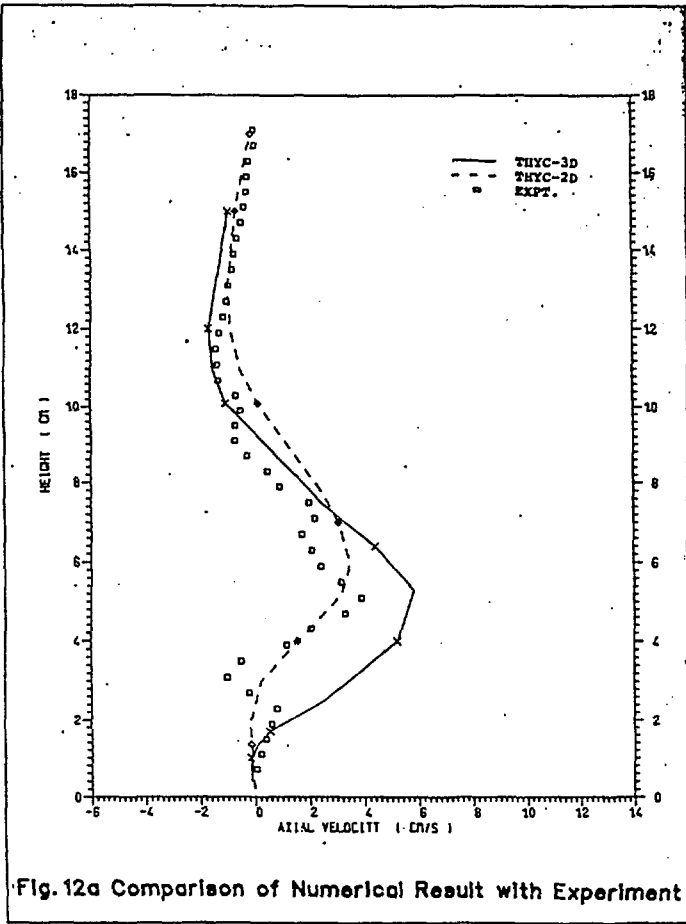


Fig. 11b Hot Pool Axial Temperature Distribution  
in RAMONA (Calculation)





121



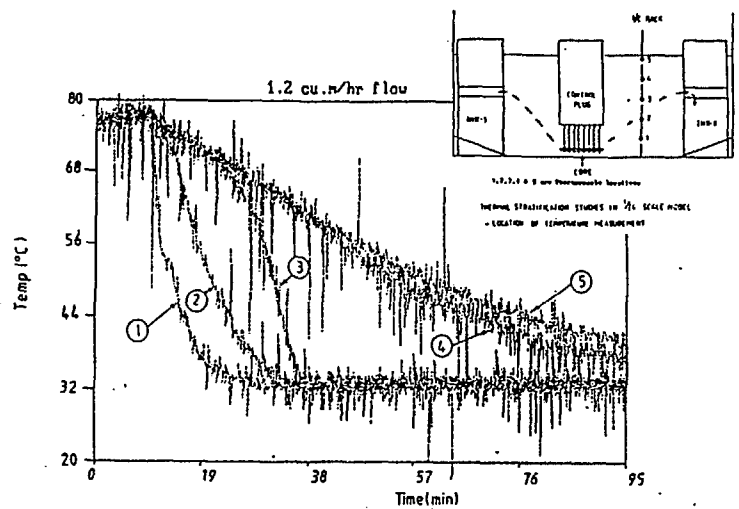


Fig. 14 Temperature Evolution in the Hot Pool at ...  
5% of Cold Water Flow (Experiment)

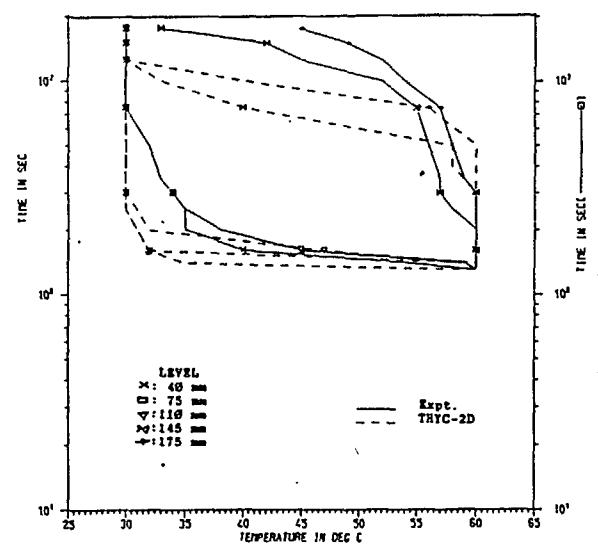


FIG. 15 STRATIFICATION STUDIES IN 1/24 SCALE MODEL OF PFR  
( 8 Cu.m/hr to 2 Cu.m/hr )

122